Late Eocene to Quaternary deformation and stress field evolution of the Orava region (Western Carpathians)

IVANA PEŠKOVÁ[1], RASTISLAV VOJTKO[1], DUŠAN STAREK[2] AND ĽUBOMÍR SLIVA[1]

[1]*Department of Geology and Paleontology, Faculty of Natural Sciences, Comenius University, Mlynská dolina, pav. G, 842 15 Bratislava, Slovakia.*
E-mails: vojtko@fns.uniba.sk, peskova@fns.uniba.sk, sliva@fns.uniba.sk
[2]*Geological Institute of the Slovak Academy of Sciences, Dúbravská cesta 9, 842 28 Bratislava, Slovakia.*
E-mail: dusan.starek@savba.sk

ABSTRACT:

Pešková, I., Vojtko, R., Starek, D and Sliva, L. 2009. Late Eocene to Quaternary deformation and stress field evolution of the Orava region (Western Carpathians). *Acta Geologica Polonica*, **59** (1), 73–91. Warszawa.

The northern part of the Western Carpathians suffered polyphase deformation at the boundary between their Central and Outer parts. Palaeostress analysis in the Orava region revealed the existence of five different stress fields in the period from the Late Eocene to the Quaternary. The evolution of the stress fields was determined by detailed structural analysis of the fault slip and fold orientation data. The orientation of the stress fields shows an apparent clockwise rotation from the Late Eocene to the Quaternary. During the Late Eocene to Oligocene, E–W compression and perpendicular tension affected this area. This was the time when the Central Carpathian Palaeogene Basin formed. After this compression, the palaeostress field rotated approximately 40–50°, and NW–SE compression and NE–SW tension took place in the Early Miocene. The Middle Miocene to Pliocene was characterised by progressive rotation of the palaeostress field from NW–SE to the NE–SW direction of the maximum principal compressional stress axis (σ_1). This clockwise rotation of the Oligocene to Quaternary palaeostress fields here is explained by the effect of the counterclockwise rotation of the ALCAPA microplate, and by the regional stress field changes in this region. The Quaternary stress field was reconstructed on the basis of structural measurements in the Pliocene sedimentary formations of the Orava–Nowy Targ Basin. The results of the palaeostress analysis show that the Quaternary stress field is characterised by E–W-oriented S_h (minimum horizontal compression) and N–S-oriented S_H (maximum horizontal compression).

Key words: Structural geology; Cenozoic; Paleogene; Faulting and folding; Central Carpathian Palaeogene Basin; Western Carpathians; Fault slip data; Palaeostress analysis.

INTRODUCTION

The orientation of the principal stress axes was studied in the Late Eocene to Early Miocene and Pliocene sedimentary formations of the Central Carpathian Palaeogene Basin (CCPB) and also of the Orava–Nowy Targ Basin (ONTB). The palaeostress analysis was based on fault geometry and fold orientation investigations. Study of the palaeostress field and orientation of the prin-

cipal palaeostress axes plays an essential role in the interpretation of the geodynamics of the Carpathian orogen.

During the last two decades, several studies have been published on the Cenozoic stress field evolution of the Alpine–Carpathian–Pannonian area (Ratschbacher *et al.* 1991; Csontos *et al.* 1991; Fodor 1995; Marko *et al.* 1995; Hók *et al.* 1995; Marko and Kováč 1996; Bada *et al.* 1996; Hók *et al.* 1998; Hók *et al.*

1999; Fodor *et al.* 1999; Marko and Vojtko 2006). These structural data, with stratigraphic, palaeogeographic, palaeomagnetic and geophysical results, were elaborated for the geodynamic evolution of the Western Carpathians and the whole Carpathian–Pannonian region during the Cenozoic (Balla 1984; Royden 1988; Csontos *et al.* 1992; Kováč *et al.* 1993; Kováč *et al.* 1994; Fodor *et al.* 1999; Kováč 2000). They suggest that the evolution of the Western Carpathians was strongly controlled by the continental escape of the ALCAPA segment from the Eastern Alps along large-scale transcurrent faults (Ratschbacher *et al.* 1991).

This paper presents the results of meso-scale structural measurements carried out in the northern part of the Central Western Carpathians. Interpretation of the data was improved by analysis of the map-scale tectonic structures, as well as by stratigraphic and sedimentary research. The palaeostress data were balanced against the palaeomagnetic data (Márton *et al.* 1992; Kováč and Márton 1998; Márton *et al.* 1999). Special emphasis was placed on the creation of a new palaeostress database for the Western Carpathians. Using these data, a detailed description of the Cenozoic to Quaternary stress field evolution and its connection with the geodynamics of the Western Carpathian arc is given.

The new results presented herein are based mainly on field observations. Systematic small- to meso-scale measurements and their statistical and palaeostress analysis were carried out. The research was focused on the northern edge of the Central Western Carpathians and the Periklippen zone, mainly in the Orava and partly in the Podhale regions.

GEOLOGICAL SETTING

The Western Carpathians extend from the eastern end of the Eastern Alps toward the northeast, and they are divided by the Pieniny Klippen Belt into the Outer and Central Western Carpathians. The Orava region has a complicated geological structure and, being located at this boundary zone, is affected predominantly by strong strike-slip deformation along this zone (Ratschbacher *et al.* 1993, Nemčok and Nemčok 1994; Kováč and Hók 1996, Plašienka *et al.* 1997).

The Outer Western Carpathians (OWC) consist predominantly of Early Cretaceous to Early Miocene flysch formations deposited on an oceanic crust (e.g. Tari *et al.* 1993; Golonka *et al.* 2005 for the pre-Oligocene evolution) and/or a thinned continental crust (e.g. Winkler and Slączka 1992). During the Late Oligocene to Middle Miocene subduction, the flysch formations were detached from their basement and thrust northward over the European Platform (Książkiewicz 1977; Oszczypko and Slączka 1989; Kováč *et al.* 1993; Plašienka *et al.* 1997; Kováč 2000) (Text-fig. 1).

The Pieniny Klippen Belt is a large-scale narrow shear zone forming the boundary which separates the accretionary wedge of the Outer Western Carpathians and the Central Western Carpathians (Ratschbacher *et al.* 1993; Nemčok and Nemčok 1994). This zone is composed of the Kysuce, Czorsztyn, Orava and Klape successions, and is formed from Jurassic to Cretaceous rocks (Birkenmajer 1986). The deformation began during the Late Cretaceous (documented by synorogenic flysch formation), but the main brittle deformation in the Pieniny Klippen Belt occurred during the Palaeogene to Neogene. The Eocene to Oligocene was characterized by
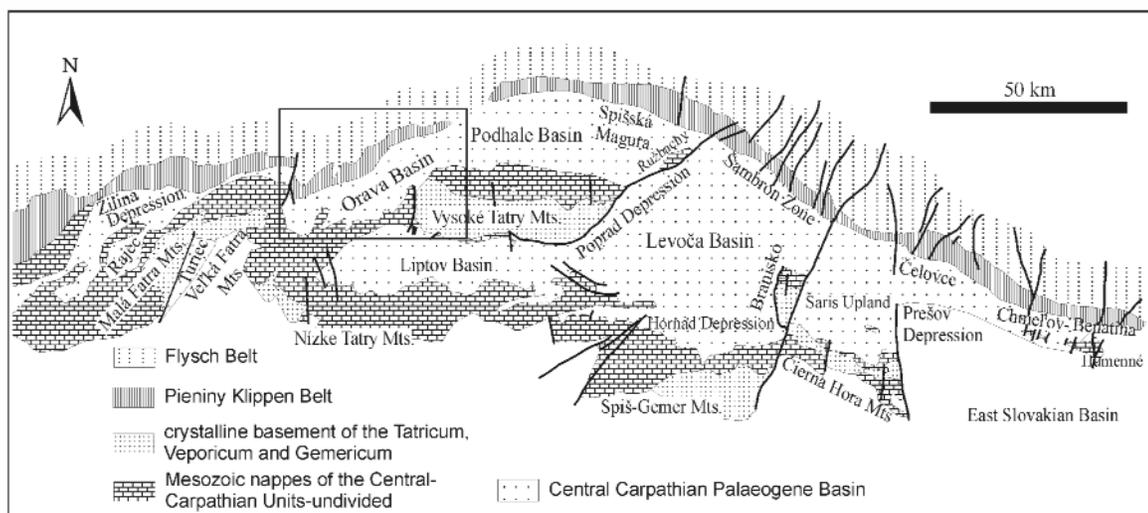
Text-fig. 1. Simplified tectonic sketch map of the northern part of the Central Western Carpathians according to Lexa *et al.* (2000). Study area is shown by rectangle

dextral transpression which altered to a Neogene sinistral transpression and then to a transtensional tectonic regime (Fodor 1995; Kováč 2000).

Most of the Orava territory is located in the Central Western Carpathians (CWC) which is composed of the Tatric, Fatric and Hronic units (Gross *et al.* 1993). The Tatric Unit is formed by the Variscan basement, which consists of Lower Palaeozoic metamorphic sequences (para- and orthogneisses, mica schist and migmatite). These metamorphic sequences have been intruded by Late Palaeozoic granitoids. The basement is covered by an autochthonous sedimentary sequence with a stratigraphic range from Permian to Middle Cretaceous. This Tatric structure is overthrust by the Fatric Unit (Krížna nappe), which was derived from the area between the Tatric and Veporic realm (Plašienka 1999, 2003). It consists mainly of Triassic to Middle Cretaceous sedimentary sequences. The age of the thrusting is documented by the deposition of synorogenic flysch (the Poruba Formation) during the Albian to Early Turonian, and by the age of the youngest deposition in the Tatric cover sequences (Plašienka 1999, 2003). The uppermost nappe structure is formed by the Hronic Unit (Choč nappe) which consists predominantly of carbonate sequences with a stratigraphic range in the Vysoké Tatry Mts. from Triassic to Jurassic. These

nappes form a basement to the Eocene to Early Miocene sedimentation of the CCPB or Podhale Basin in Polish terminology (Gross *et al.* 1993).

The Orava region is composed mainly of sedimentary formations of the CCPB (Text-fig. 1). It is a postnappe structure of the CWC. This basin was formed as a marginal sea of the Peri-Tethyan Basin. It shows a forearc basin position developed on the destructive platemargin and behind the Outer Carpathian accretionary wedge (Tari *et al.* 1993; Soták *et al.* 2001). The CCPB sediments in the Orava region are interpreted as facies system tracts alternating in time during the evolution of the basin, and corresponding to tectonic, climatic and sea-level changes (Starek 2001).

The sedimentary deposition of the CCPB in the Orava region is commonly divided into the lithostratigraphic formations of the Subtatric Group defined by Gross *et al.* (1984) (Text-fig. 2). The Borové Formation is a transgressive lithofacies consisting of breccia, conglomerate, polymict sandstone to siltstone, organodetrital to organogenic limestone and marlstone. In the uppermost part of the formation alluvial and deltaic sediments of the Pucov Member are locally preserved. The Huty Formation (Zakopane Formation) is composed of non-calcareous claystone of the Menilite type overlain by calcareous claystone lithofacies with fine- to mediumgrained sandstone. The overlying Zuberec Formation (Chocholów Formation) reflects increasing sediment supply to the basin and is composed of typical flysch sediments. The uppermost part of the Subtatric Group is formed from the Biely potok Formation (Ostryzs Formation), characterized by sediments with a predominance of medium- and coarse-grained massive sandstone banks. This formation represents the beginning of the final stage of the sedimentary history of the basin; the youngest sediments are not preserved due to subsequent basin inversion. The time-span of the Subtatric Group was stated to be Lutetian to Early Oligocene (Gross *et al.* 1984, 1993). However, the nannoplankton evidence indicates that the upper limit of this range needs to be revised to latest Oligocene or even Early Miocene (Soták *et al.* 1996; Soták 1998; Olszewska and Wieczorek 1998; Starek 2001).

The Orava–Nowy Targ Basin originated after the Early Sarmatian (Nagy *et al.* 1996). The infill of this depression consists of Karpatian to Badenian coarsegrained sandstone, claystone, and intercalations of lignitic claystone, Sarmatian grey claystone and siltstone with lignite. It also contains Pliocene greenish-grey claystone and siltstone with intercalations of sandstone. The Orava–Nowy Targ Depression was previously considered to be a retro-arc basin (Roth *et al.* 1963). However, because it is situated along the Periklippen shear zone,
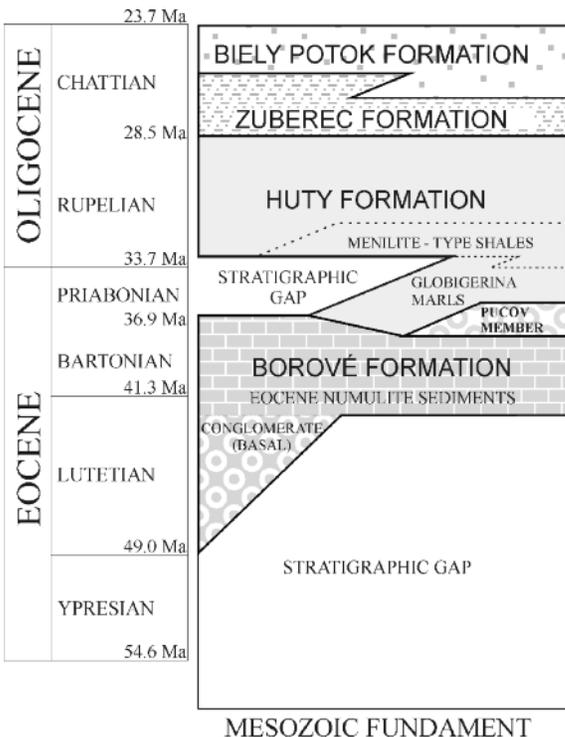
Text-fig. 2. Stratigraphic column of the Central Carpathian Palaeogene Basin formations according to Gross *et al.* (1984) and Starek (2001); modified

this depression is currently considered to be a pull-apart structure (Pospíšil 1990; Pomianowski 2003).

METHODS

The palaeostress reconstruction of the Orava region was carried out by a systematic collection of meso-scale structural elements. Observations were made on the striated fault surfaces, extensional veins, stylolites, folds and all additional structures with reference to the type of the faults, the direction, sense of shearing, and the quality of displacement measurement. The quality ranking scheme according to the World Stress Map project from A (best) to E (worst) as a function of several criteria (Sperner *et al.* 2003) was used. The basic principle of palaeostress analysis is that meso-scale structures can be related to larger regional structures; both scales reflect the same dynamics and kinematics (Angelier 1994). The sense of movement on fault surfaces can be deduced from criteria summarised by Hancock (1985), Petit (1987), Marko (1993) and Angelier (1994).

Analysis of fault slip data for the reconstruction of tectonic stresses are now routinely undertaken in tectonic investigations. Standard procedures for brittle fault slip data analysis and palaeostress reconstruction are well established (Angelier 1979, 1989, 1990, 1994; Etchecopar *et al.* 1981; Michael 1984; Delvaux and Sperner 2003). The inversion method is based on the assumption of Bott (1959) and Wallace (1951) that the slip on a plane occurs in the direction of the maximum resolved shear stress. Fault data were inverted to obtain the four parameters of the reduced stress tensor: the principal axes are σ_1 (maximum compressional stress axis), σ_2 (intermediate stress axis), σ_3 (minimum stress axis) and the ratio of the principal stress differences: $\Phi = (S_2 - S_3) / (S_1 - S_3)$. The latter defines the shape of the stress ellipsoid. The one used here is the equivalent of the ratio of Angelier (1989, 1994).

The previously mentioned basic assumption of the inversion method has limitations and hence the results of this method were disputed by some authors. In the common situation where early faults accumulate displacements and rigid rotations, and where new faults develop during progressive deformation, fault-slip data can be rather complex and variable in space, and reflect neither local stress and strain rate tensors, nor finite strains and finite rotations in a simple way (Dupin *et al.* 1993; Pollard *et al.* 1993; Nieto-Samaniego and Alaniz-Alvarez 1996; Twiss and Unruh 1998; Maerten 2000; Roberts and Ganas 2000; Gapais *et al.* 2000). The basic assumption of calculation of the reduced stress tensor from fault slips is that the regional stress tensor is spatially and chronologically homogeneous throughout the rock mass and throughout the duration of the deformation phase. The calculation can be influenced by three effects: (1) the effect of the ratio between the width and the length of a fault; (2) the effect of the Earth surface; and finally (3) the effect of interaction among faults (for further reading see Pollard *et al.* 1993). All three effects can distort the results of palaeostress analysis but their influence on results is minimal (Angelier 1994).

The crucial step in field structural research of faults was the kinematic analysis of fault slips, based on the evaluation of kinematic indicators on slickenside surfaces and on the evaluation of outcrop-scale structures genetically related to the fault dynamics. The obtained data were processed using the analytical stress method (Angelier 1989, 1994) with the TENSOR software package (Delvaux 1993; Delvaux and Sperner 2003). The first used program is called the Dieder. It is an improved version of the Right Dihedron method of Angelier and Mechler (1977). It provides an approximate determination of the four parameters of the reduced stress tensor and also allows a preliminary separation of the fault population into an homogeneous set, broadly compatible with the computed stress tensor (for further information see Delvaux 1993; Delvaux and Sperner 2003). The second one is the Shear program (Rotational Optimization) The inversion is performed using an iterative procedure, by testing a great number of different stress tensors, with the aim to minimize a misfit function. The simplest misfit function to minimize is the slip deviation a between the observed slip direction and the theoretical shear stress on the plane. This includes a function that integrates the simultaneous minimisation of normal stress and maximisation of shearing stress magnitudes on each fault plane. The Rotational Optimisation procedure allows the search area to be further restricted during the inversion, so that the whole grid does not have to be searched (Delvaux 1993; Delvaux and Sperner 2003).

The analysis of fold orientation in the CCPB and PKB sediments was carried out using meso-scale fold data, as well as bedding measurements made during geological and sedimentological research. The stress field was determined using the orientation data of bedding, fold axes and axial planes. The principal deformational axes characterize the fold geometry. The principal strain axis (A) is parallel to the direction of the maximum elongation, the principal strain axis (C) is parallel to the direction of the shortening, and the principal strain axis (B) is parallel to the direction of the fold axis (Michael 1984). The geometry of the folds roughly defines the relationships of the orienta-

tion of the palaeostress axes. Fold axes and fold planes are generally perpendicular to the maximum principal palaeostress axis σ_1 in simply folded regions. Macro-fold axes and axial planes were constructed from measured fold limbs using the π pole method (construction of β axes). Fold orientation, statistics and separation were computed and visualized with the Fabric 7 software. The principles of these methods are described in Wallbrecher (1986).

RESULTS OF STRUCTURAL ANALYSIS

The deformational history of the Orava region is characterised by polyphase brittle faulting and accompanying semi-brittle flexural slip folding (Gross *et al.* 1993). The reconstructions of the stress field evolution were solved by fault slip and fold analysis in the Upper Eocene, Oligocene, Lower Miocene, and Pliocene sedimentary sequences. In total approximately 500 structural data were measured in 14 different sites (Table 1). We were able to define five different deformational phases which were considered to be the most important for understanding of the Cenozoic palaeostress evolution of the area investigated. The results of the structural analysis are listed in Tables 2 and 3 and shown graphically in Text-figs 3 a-h; 5 a-f; 6; 7; 10; 11; 12.

Fault slip analysis and palaeostress reconstruction

The five different palaeostress orientations were detected from more than 41 computed reduced stress tensors. One of them is Palaeogene, three Neogene and one is Plio–Quaternary age. The relative chronology of the Neogene palaeostress phases was deduced from overprinting relationships in a few outcrops and was also compared with deformational stages in other areas of the CWC and Pannonian Basin because these areas show an Oligocene to Quaternary evolution comparable to that of the Orava region (Kováč and Hók 1996; Fodor *et al.* 1999). The palaeostress results and the chronology (Text-fig. 4) of faulting are described from the oldest to the youngest deformational phases.

E–W compression – N–S tension (Late Eocene–Earliest Miocene)

The earliest deformational phase which affected the Orava region is predominantly characterized by a ENE–WSW-trending dextral strike-slip and WNW–ESE-trending sinistral strike-slip faults. The oblique reverse faults were partly observed. Most of the measured fault slip data were interpreted as neoformed fault structures on the basis of their plane symmetry (conjugate faults). The faults belonging to the earliest phase are weakly preserved in the older formations (the Borové and Huty formations) of the CCPB. We proposed that the faults are younger than the deposition of the Borové and Huty Formations, and older than the Zuberec Formation, because they cut the older strata and do not continue into the younger strata (the Zuberec and Biely potok formations). The calculated reduced stress tensor (Φ) is characterized by a E–W-oriented horizontal principal compressive stress axis (σ_1) and a N–S-oriented horizontal minimum principal stress axis (σ_3). Generally, the faults were activated under a strike-slip tectonic regime (Text-figs 3a; 6; Tables 2, 3).

NW–SE compression (Early Miocene)

The neoformed reverse and inherited oblique–reverse faults were activated during this distinct compressive phase, which was characterised by NW–SE-trending compression. The strikes of the gently-dipping fault planes trend generally NE–SW and the fault planes show nearly perpendicular slickenside lineations. The most usual position of the maximum principal stress axis (σ_1) and intermediate principal stress axis (σ_2) is approximately horizontal, unlike the minimum principal stress axis (σ_3), which is in a subvertical position. The compressive tectonic regime prevailed throughout the whole area; however, the maximum intensity of deformation was concentrated along the PKB and the northwestern margin of the Malá Fatra Mts., Chočské vrchy Mts. and Vysoké Tatry Mts. This phase is predominantly characterized by NE–SW reverse faults which are connected with reverse faulting (see Interpretation). The Huty and Huty – Kvačianska dolina localities are very good example of this deformational phase (Text-figs 3b, c; 7; 8, 9a, b; Tables 2, 3).

The deformational subphase (see Interpretation) is characterised by NNW–SSE-trending oblique normal faults. The maximum principal stress axis (σ_1) is in a subvertical position, while the minimum principal stress axis (σ_3) and intermediate principal stress axis (σ_2) are in a subhorizontal position. The faults were activated on the inherited planes under the NE–SW-oriented tension and they are weakly preserved in the sedimentary sequences of the CCPB (Text-fig. 7; Tables 2, 3).

N–S compression – E–W tension (Middle Miocene)

The most clearly marked structures are predominantly E–W-trending reverse faults; a NW–SE to
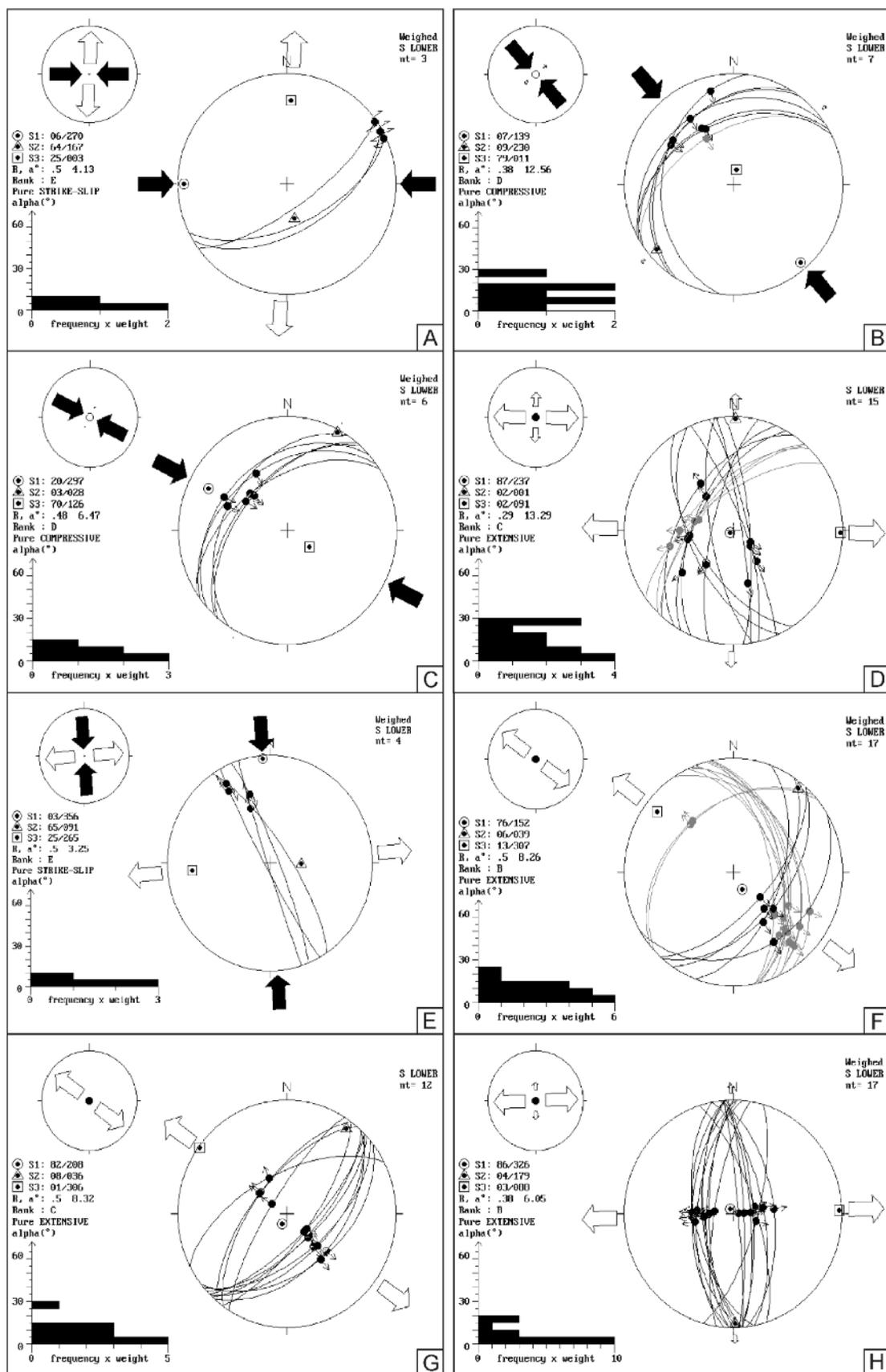
Code	Name of site	Latitude	Longitude	Formation
CCP-M	Medzihradné quarry	N49°12'02"	E019°19'28"	Borové Formation
CCP-HM	Huty – Matiašovce	N49°12'10"	E019°33'27"	Borové Formation
CCP-HKD	Huty – Kvačianska dolina	N49°12'13"	E019°32'57"	Borové Formation
CCP-P	Pucov	N49°13'18"	E019°22'11"	Huty Formation
CCP-PS	Pucov – rubbish dump	N49°13'20"	E019°22'04"	Huty Formation
CCP-H	Huty	N49°13'06"	E019°33'54"	Huty Formation
CCP-HNH	Huty - Our Hill	N49°13'25"	E019°34'28"	Huty Formation
CCP-K	K ňažia	N49°14'03"	E019°19'21"	Huty Formation
CCP-Z	Zakopane	N49°16'51"	E019°57'25"	Huty Formation
CCP-HBD	Habovka – Blatná dolina	N49°16'33"	E019°39'07"	Huty Formation
CCP-HL	Horná Lehota	N49°14'58"	E019°24'31"	Zuberec and Biely potok formations
CCP-TDI	Tichá dolina Valley I.	N49°17'03"	E019°46'39"	Zuberec and Biely potok formations
CCP-TDII	Tichá dolina Valley II.	N49°17'19"	E019°46'12"	Zuberec and Biely potok formations
NS-ONP	Lipnica Wielka	N49°27'55"	E019°37'37"	Pliocene sediments

Table 1. General information and location of sites with measured structures

Text-fig. 4. Synthetic table of chronology for Late Eocene to Quaternary regional stress fields in the Orava region

Text-fig. 3. Examples of palaeostress reconstructions for the Orava region. (a) Late Eocene–Earliest Miocene phase recorded at the Huty – Our Hill locality (site code CCP-HNH1); S_0 – 329/41°. (b) Early Miocene phase; the Huty locality (site code CCP-H1); S_0 – 322/32°. (c) Early Miocene phase; the Huty – Kvačianska dolina locality (site code CCP-HKD1); S_0 – 338/33°. (d) Middle Miocene phase; the Huty – Matiašovce locality (site code CCP-HM3); S_0 – 338/20°. (e) Middle Miocene phase; the Pucov locality (site code CCP-P1); S_0 – 123/18°. (f) Late Middle to Late Miocene phase; the Pucov rubbish dump (site code CCP-PS1); S_0 – 23/7°. (g) Late Middle to Late Miocene phase; the Oravice – Tichá dolina II (site code CCP-TDII.1); S_0 – 356/23°. (h) Pliocene to Quaternary phase; the Lipnica Wiełka (site code NS-ONP1). Explanation: Stereogram (Schmidt net, lower hemisphere) with traces of fault planes, observed slip lines and slip senses, histogram of observed slip-theoretical shear deviations for each fault plane and stress map symbols. $S_1 = \sigma_1$, $S_2 = \sigma_2$ and $S_3 = \sigma_3$ – azimuth and plunge of principal stress axes; $R = \Phi$ – stress ratio (S_2–S_3/S_1–S_3); α – mean slip deviation (in °), Rank – quality ranking scheme according to World Stress Map project from A (best) to E (worst) as a function of several criteria (Sperner *et al.* 2003), and S_0 – bedding

NNW–SSE right-lateral strike-slip, and generally NE–SW left-lateral strike-slip faults. The maximum principal stress axis (σ_1) and the minimum principal stress axis (σ_3) are approximately horizontal, unlike the intermediate compressional axis (σ_2). Small-scale extensional structures such as tension gashes, veins with calcite fibres, etc., with an approximately N–S strike were also observed. This deformational phase occurred in many localities with a prevailing strike-slip tectonic regime (e.g. The Huty – Matiašovce locality) (Text-figs 3d, e; 9c; 10; Tables 2, 3).

NW–SE tension – NE–SW compression (Late Middle to Late Miocene)

This deformational phase affected the Orava region during the Late Miocene and was characterized by NW–SE tension which replaced the previous compressional strike-slip tectonic regime. The main structural elements
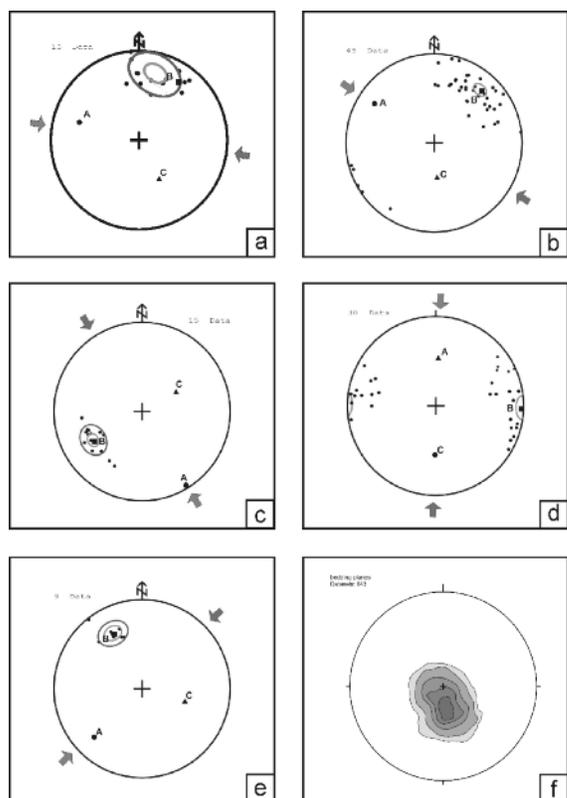
Text-fig. 5. Distribution of the β axes from meso-scale fold structure (Schmidt projection, lower hemisphere). Examples from the localities: (a) the Habovka – Blatná dolina (site code CCP-HBDV1); (b) the Huty (site code CCP-HV2); (c) the Huty (site code CCP-HV1); (d) the Zakopane (site code CCP-ZV2); (e) the Huty (site code CCP-HV4). (f) Contour plot of poles of the bedding planes; contour intervals (1, 3, 6, 9, 12%) are calculated by the 1%-counting circle method and maximum value is 13.8% at S_0 0/24˚

are predominantly NE–SW-trending normal faults at the beginning of this phase and NNE–SSW dextral strike-slip and ENE–WSW sinistral strike-slip faults. Nice examples documenting this extensive tectonic regime have been observed at the Pucov rubbish dump (Text-fig 9d) and the Oravice–Tichá dolina II. These structures cut the whole sequence of the CCPB, but they do not continue to the Pliocene sedimentary formations of the Orava–Nowy Targ Basin (Text-figs 3f, g; 11; Tables 2, 3).

E–W tension (Pliocene – ? Quaternary)

The youngest deformational phase recorded from the fault slip data was E–W extension. The maximum principal stress axis (σ_1) was generally vertical, while the σ_2 and the σ_3 axes were subhorizontal. The most pronounced structural elements of this deformational phase are the N–S-trending normal faults. These normal faults were activated as conjugate sets. The faults were measured mostly in the Pliocene sediments of the Orava–Nowy Targ Basin and also in the Borové and Huty formations of the CCPB. This tectonic regime led to the evolution of neoformed conjugate fault structures in the Pliocene sediments, and neoformed conjugate slips or inherited faults (weakness planes) in the Palaeogene sediments. In total, 17 faults were measured in the Lipnica Wielka sandpit; the fault slips were activated under an almost pure extensive tectonic regime. The kinematics of the normal faults was determined on the basis of sedimentary marker offsets along striae, polished versus striated facets on these fault planes but they do not contain mineral fibres. The similarly oriented normal fault planes belong to the N–S compression and W–E tension phases (Middle Miocene), however these faults are characterised by mineral accretionary steps of calcite (Text-figs 3h, 12; Tables 2, 3).

Fold analysis

The folding in the Orava region was caused by flexural slip folding under semi-brittle conditions during the Neogene (Plašienka *et al.* 1998). The folds affected predominantly the deep water sedimentary sequences (Huty and Zuberec formations) of the CCPB. The observed fold tightness is generally open to closed, with the exception of that alongside the PKB and the southeastern margin of the CCPB in the Orava region, where tight folds occurred. Several measured folds with SE vergence represent back-folding in the Carpathian orogen (see Interpretation). Data obtained from the struc-

Stage 1: Late Eocene to Earliest Miocene W–E compression and N–S tension

Site	n	n_T	S_1	S_2	S_3	R	α	Q	R'	Method
CCP-HM5	4	46	116/21	300/68	207/02	0.47	5.65	E	1.53	Shear
CCP-PS5	1	36	102/50	193/01	204/40	?	?	E	?	Dieder
CCP-HNH1	3	4	270/06	167/64	003/25	?	?	E	?	Dieder
CCP-Z1	5	25	255/30	032/52	152/22	0.50	12.07	E	1.50	Shear

Stage 2: Early Miocene NW–SE compression and NE–SW tension

Site	n	n_T	S_1	S_2	S_3	R	α	Q	R'	Method
CCP-HM1	9	46	153/14	350/75	244/04	0.61	9.49	D	1.39	Shear
CCP-HM4	4	46	300/33	035/07	135/56	0.25	13.50	E	2.25	Shear
CCP-HKD1	6	9	297/20	028/03	126/70	0.48	6.47	D	2.48	Shear
CCP-P3	5	15	335/23	179/66	068/09	0.50	5.57	E	1.50	Shear
CCP-PS2	5	36	315/65	146/25	054/04	0.41	10.42	E	0.41	Shear
CCP-H1	7	26	139/07	230/09	011/79	0.38	12.56	D	2.38	Shear
CCP-H3	4	26	306/83	120/07	210/01	0.50	15.10	E	0.50	Shear
CCP-K1	4	5	112/18	203/02	298/71	0.46	1.25	E	2.46	Shear
CCP-Z5	5	25	136/62	315/28	226/00	0.50	13.33	E	0.50	Shear
CCP-HBD1	5	6	308/15	217/04	113/74	0.44	1.90	E	2.44	Shear
CCP-HL1	1	1	135/13	227/07	345/75	?	?	E	?	Dieder
CCP-TDI.2	4	11	299/11	029/01	127/79	0.50	5.68	E	2.50	Shear
CCP-TDII.2	4	33	131/18	222/02	317/72	0.61	3.05	E	2.61	Shear
CCP-TDII.4	2	33	218/74	309/00	039/16	?	?	E	?	Dieder

Stage 3: Middle Miocene N–S compression and E–W tension

Site	n	n_T	S_1	S_2	S_3	R	α	Q	R'	Method
CCP-HM2	6	46	210/20	065/65	305/13	0.38	8.55	D	1.62	Shear
CCP-HM3	15	46	237/87	001/02	091/02	0.29	13.29	C	0.29	Shear
CCP-P1	4	15	356/03	091/65	265/25	0.50	3.25	E	1.50	Shear
CCP-PS4	6	36	018/38	174/50	279/12	0.40	11.45	D	1.60	Shear
CCP-H4	3	26	195/22	298/28	072/53	?	?	E	?	Dieder
CCP-H5	5	26	205/03	296/05	078/84	0.50	4.20	E	2.50	Shear
CCP-K2	1	5	002/09	092/01	188/81	?	?	E	?	Dieder
CCP-Z2	4	21	163/21	026/63	260/17	0.46	1.08	E	1.54	Shear
CCP-Z4	5	25	349/27	258/01	166/63	0.50	3.58	E	2.50	Shear
CCP-TDI.3	2	11	359/25	190/65	097/01	?	?	E	?	Dieder

Stage 4: Late Middle - Late Miocene NW–SE tension and NE–SW compression

Site	n	n_T	S_1	S_2	S_3	R	α	Q	R'	Method
CCP-M1	7	7	345/69	208/16	114/13	0.43	5.24	D	0.43	Shear
CCP-HKD3	1	9	248/03	151/62	340/27	?	?	E	?	Dieder
CCP-P2	6	15	006/84	214/05	124/03	0.50	7.55	D	0.50	Shear
CCP-PS1	17	36	152/76	039/06	307/13	0.50	8.26	B	0.50	Shear
CCP-PS3	5	36	264/73	023/08	115/15	0.46	6.24	E	0.46	Shear
CCP-H2	6	26	096/71	226/13	319/14	0.48	5.57	D	0.48	Shear
CCP-Z3	3	25	157/59	055/07	321/30	?	?	E	?	Dieder
CCP-HBD2	1	6	063/22	153/01	244/68	?	?	E	?	Dieder
CCP-TDI.1	3	11	163/62	063/05	330/27	?	?	E	?	Dieder
CCP-TDII.1	12	33	208/82	036/08	306/01	0.50	8.32	C	0.54	Shear

Stage 5: Pliocene - (?)Quaternary E–W tension

Site	n	n_T	S_1	S_2	S_3	R	α	Q	R'	Method
NS-ONP1	17	18	326/06	179/86	088/03	0.38	6.05	B	0.38	Shear
CCP-HKD2	2	9	282/69	013/00	103/21	?	?	E	?	Dieder
CCP-HBD3	2	6	215/76	010/12	101/06	?	?	E	?	Dieder

Table 2. Palaeostress tensors from fault slip data. Explanations: Site – locality code; n – number of fault used for stress tensor determination; n_T – total number of fault data measured; $S_1 = \sigma_1$, $S_2 = \sigma_2$ and $S_3 = \sigma_3$ – azimuth and plunge of principal stress axes; R = Φ – stress ratio (S_2–S_3/S_1–S_3); α – mean slip deviation (in °); Q – quality ranking scheme according to the World Stress Map Project (Sperner *et al.* 2003); R' – tensor type index as defined in the text; method – method used

Site	n	n_T	A	B	C
CCP-HKDV1	7	9	172/24	054/47	279/33
CCP-PSV1	3	6	312/32	049/12	157/55
CCP-PSV2	3	6	056/05	326/09	180/84
CCP-HV1	15	96	149/01	240/36	057/54
CCP-HV2	45	96	303/18	041/23	178/60
CCP-HV3	11	96	192/06	283/16	083/73
CCP-HV4	9	96	227/24	332/30	105/50
CCP-HNHV1	5	14	88/23	190/27	323/53
CCP-KV1	4	4	155/15	056/03	310/79
CCP-ZV1	3	36	77/35	319/34	199/37
CCP-ZV2	30	36	183/46	092/01	001/44
CCP-HBDV1	15	23	287/28	031/23	153/52
CCP-HBDV2	4	23	355/07	263/16	117/72
CCP-TDI.V1	3	5	200/11	294/21	084/66
CCP-TDII.V1	4	15	282/01	012/19	191/71
CCP-TDII.V2	5	15	333/21	066/08	177/67
CCP-TDII.V3	2	15	337/01	307/12	127/18

Table 3. Orientation of principal fold axes. Explanations: Site – locality code; n – number of fold data used for determination of stress orientations; n_T – total number of fold data measured; A – axis of maximum elongation, B – intermediate axis (fold axis) and C – axis of maximum shortening
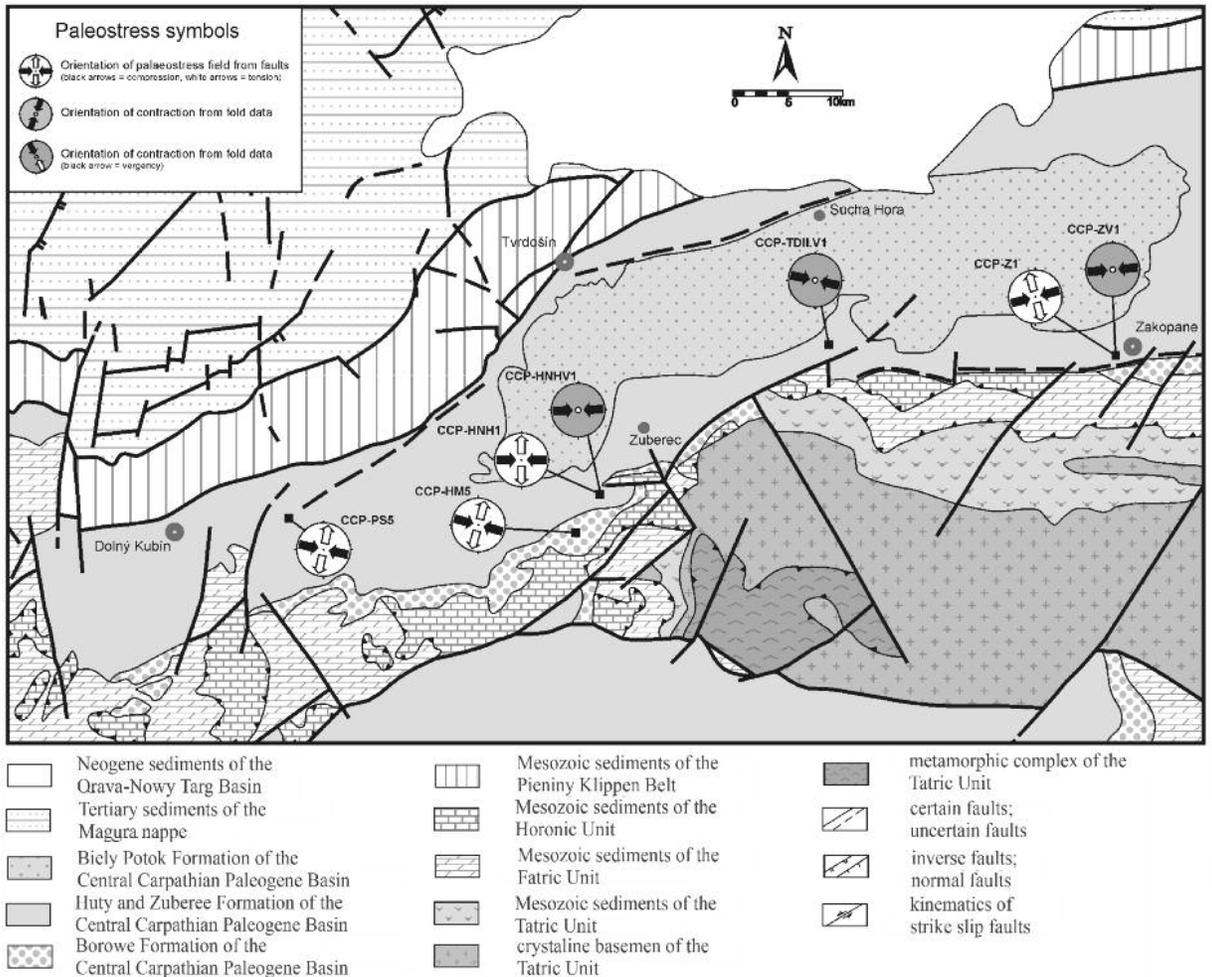
Text-fig. 6. Simplified tectonic map with orientation of palaeostress symbols of the W–E compression and N–S tension (Late Eocene–Earliest Miocene). For additional information on localities and computed reduced stress tensors see Tables 2 and 3 and for the locations of the localities see Table 1 according to site codes

tural analysis of the folds indicate the presence of four main deformational stages with N–S, NE–SW, E–W and NW–SE trending β fold axes (calculated from both bedding attitude and measurements of axes) (Text-fig. 5).

INTERPRETATION AND DISCUSSION

The convergence of the Adria Microplate and the European Platform during the Eocene to Miocene induced evolution of the palaeostress field orientation in the area
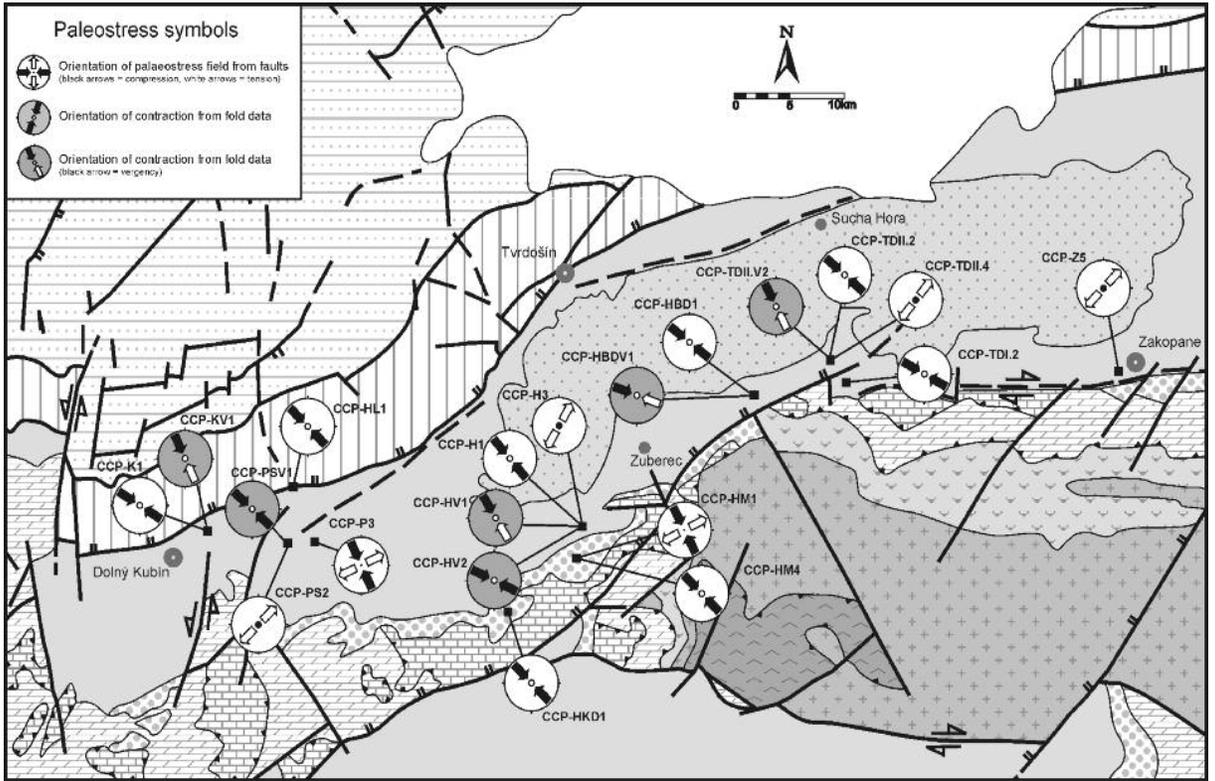
Text-fig. 7. Simplified tectonic map with orientation of palaeostress symbols of the NW–SE compression and NE–SW tension (Early Miocene); see Tables 2 and 3
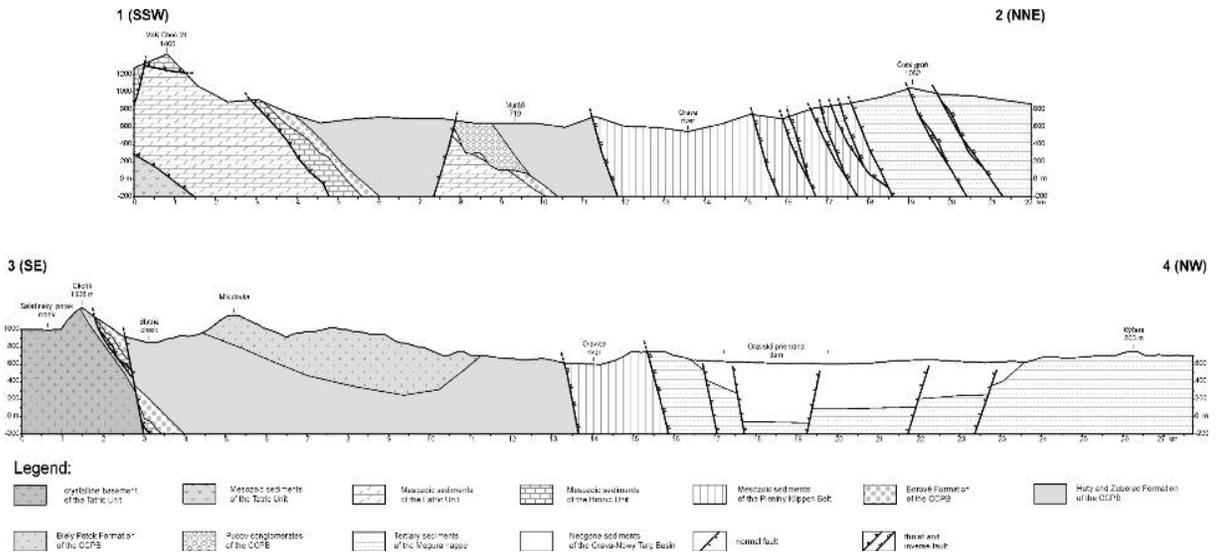
Text-fig. 8. Schematized geological cross-sections of the Orava region (not to scale). For the positions of the geological cross-sections see Text-fig. 1

investigated. The area is located on a convergent plate margin which existed along the external part of the CWC edge during the whole of the Palaeogene. The typical flysch sedimentation affected not only the lower oceanic plate (the Magura Basin) but also the frontal part of the overriding continental plate (CCPB). The flexure was most likely generated by subcrustal erosion of lower crustal oceanic elements accreted to the upper plate during the preceding subduction period (Wagreich 1995), and/or by trench suction and subduction zone roll-back effects (Plašienka *et al.* 1997). This subduction process resulted in the closure and destruction of the Palaeogene forearc basin above the active CWC thrust front during the Early Miocene. The CCPB was formed as a marginal basin of the Paratethys. It shows a forearc position extended on the destructive plate margin and behind the Outer Carpathian accretionary wedge (Soták and Starek 2000; Soták *et al.* 2001). Destruction and inversion of the

CCPB is dated as Early Miocene because the youngest known sediments are Egerian–Eggenburgian in age (Soták *et al.* 2001). The youngest sediments of the Magura nappe in the OWC have the same age (Oszczypko *et al.* 2005). However, we have to calculate that some of the highest strata of the Magura Basin and the CCPB were already missing because of erosional processes after basin inversion.

The reconstruction of the Oligocene to Quaternary palaeostress field of the area was carried out by structural measurements of fault slip data and fold plane and axis orientations.

The E–W compression and perpendicular tension is considered to be the oldest deformational phase recorded in the Upper Eocene to Oligocene sedimentary sequences of the CCPB. This deformation is weakly preserved in the older formation of this basin (Text-figs 3a; 5a; 6) and also in the Central Western Carpathians, e.g.
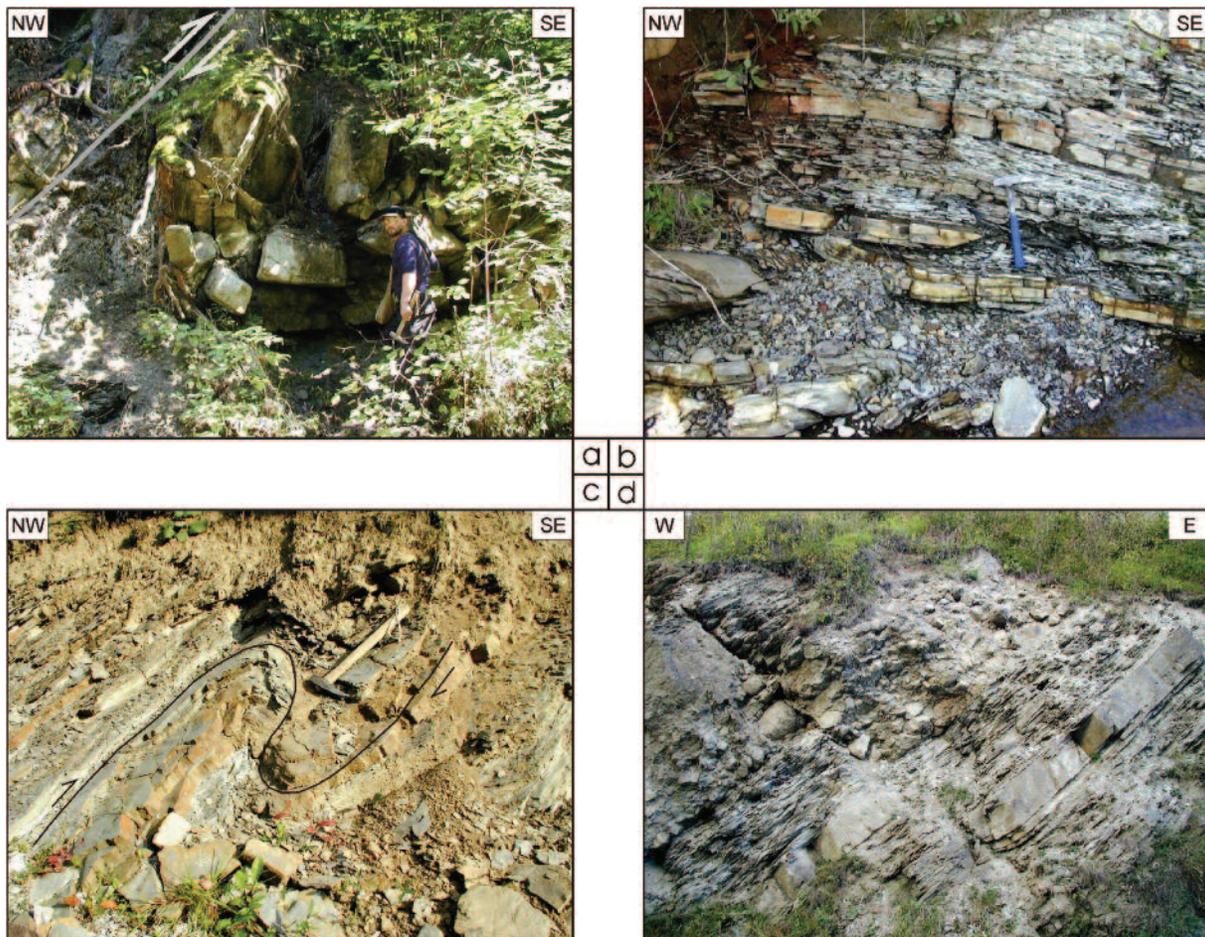
Text-fig. 9. Field photos of the observed tectonic structures. (a) The Horná Lehota locality; asymmetric fold with SE vergence during reverse faulting. Mesozoic rocks of the Pieniny Klippen Belt are located above the reverse fault and the folded Oligocene sediments of the CCPB can be seen below the fault (b) The Huty locality; small reverse faulting in the Huty Fm. with SE vergence. (c) Huty–Kvačianska dolina locality; well developed asymmetric fold in the Zuberec Fm. (d) Pucov rubbish dump locality; well developed normal faults in the Pucov Mb. The kinematics of the faults has been determined on the basis of stratigraphic marker offsets and drag folds
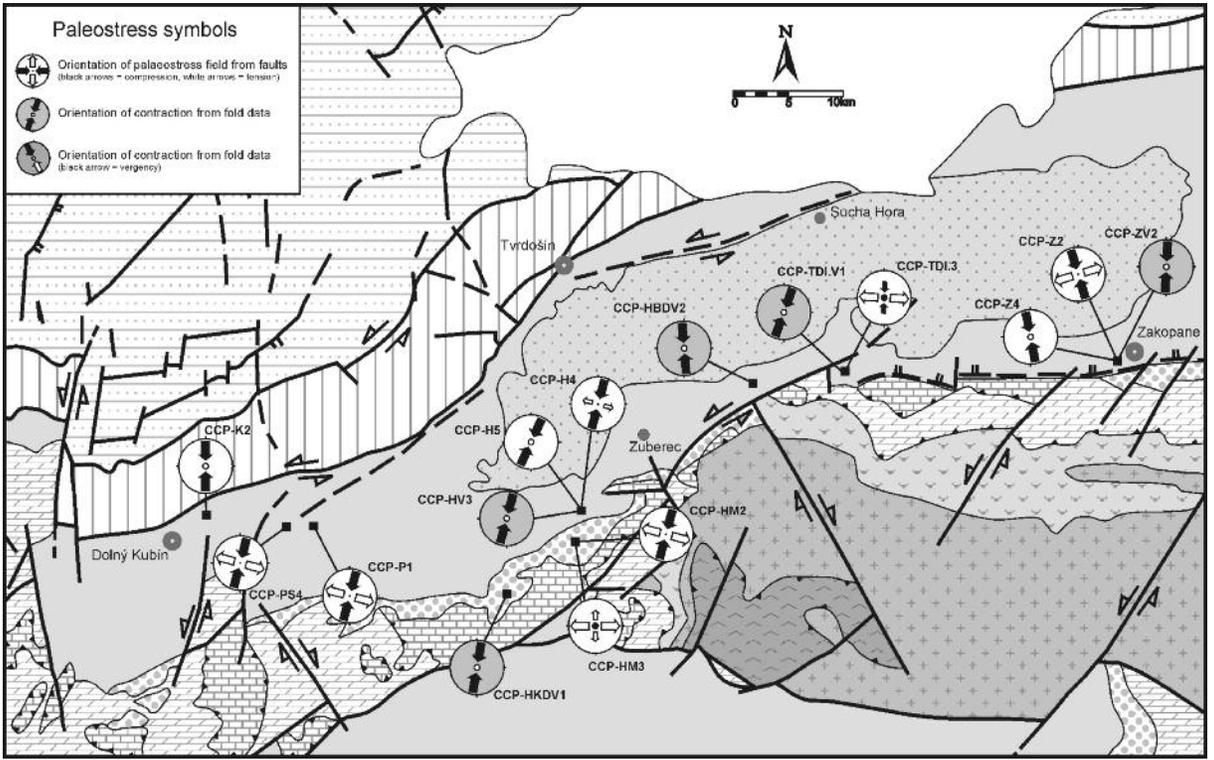
Text-fig. 10. Simplified tectonic map with orientation of palaeostress symbols of the N–S compression and W–E tension (Middle Miocene); see Tables 2 and 3
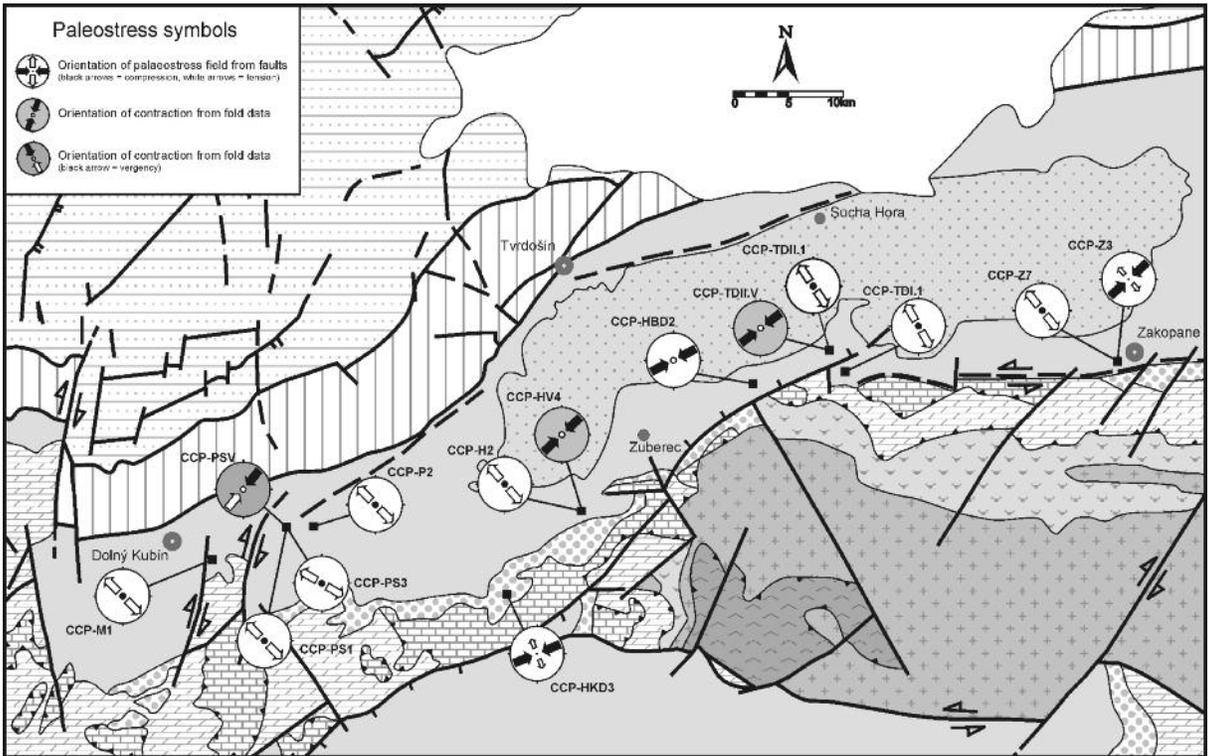
Text-fig. 11. Simplified tectonic map with orientation of palaeostress symbols of the NE–SW compression and NW–SE tension (Late Miocene); see Tables 2 and 3

in the Vysoké Tatry Mts. (Tokárová 2004), in the Sloven-ské rudohorie Mts. (Vojtko 2003), and in the entire hinterland (Fodor *et al.* 1992, 1999; Marko *et al.* 1995). If the Miocene rotations of approximately 80° are considered (Márton *et al.* 1992; Kováč and Márton 1998; Márton *et al*. 1999), the original orientation of the maximum compressional axis (σ_1) was generally in the N–S direction. The stress field reflects the Meso-Alpine convergence of the Adriatic and European microplates (Ratschbacher *et al*. 1991; Csontos *et al.* 1992; Csontos 1995; Fodor *et al.* 1999; Kováč 2000). However, precise data on the palaeostress orientation and character of the tectonic regime during the evolution of the CCPB are still not available. At several localities, the sediments were also disturbed by folding with N–S-trending fold axes. This fold orientation confirms the E–W direction of maximum compression.

During the Early Miocene, the orientation of the maximum compressional stress axis (σ_1) was in the NW–SE direction. In reality, this NW–SE compression is the first deformation that is pervasively visible throughout the area (Text-figs 3b, c; 5b, c; 7; 9b;). This tectonic regime is well recorded at many sites exposing the Upper Eocene to Lower Miocene sedimentary formations of the CCPB. The conspicuous NE–SW-oriented complex synclinal structure of the Orava segment of the CCPB was developed during the NW–SE compression and it plays an es-sential role in the surface distribution of the Upper Eocene to Lower Miocene formations in the CCPB. The youngest sediments of the CCPB are found in the centre of the basin (Biely potok Formation) and the oldest (Borové and Huty formations) are located around the basin margin (Text-fig. 8). At the same time, the prevailing compressive tectonic regime also caused the south vergent reverse faulting and folding of the PKB and CCPB. The reverse structures are well exposed in the Ostrý grúň brook near the village of Horná Lehota (Text-fig. 9a) and also near the villages of Kňažia and Podbieľ. The effects of the reverse faulting and folding tectonics can also be seen near the village of Zázrivá, at the southwestern border of the Orava region (Haško and Polák 1978; Marko *et al.* 2005). This compressional regime was also observed in the western part of the Western Carpathians (Kováč *et al.* 1989, 1993; Marko *et al.* 1990, 1991; Fodor 1995; Kováč 2000). An extensional tectonic regime occurred at the end of this deformational phase and is characterized by dominant NE–SW tension. This tension is poorly preserved and it is considered to be the final stage of the NW–SE compression.

The NW–SE compression rotated progressively to a N–S direction during the Middle Miocene. It is proposed that N–S compression of the strike-slip tectonic regime was caused by the migration and fixation of the Carpathian thrust front towards the northeast (Text-figs
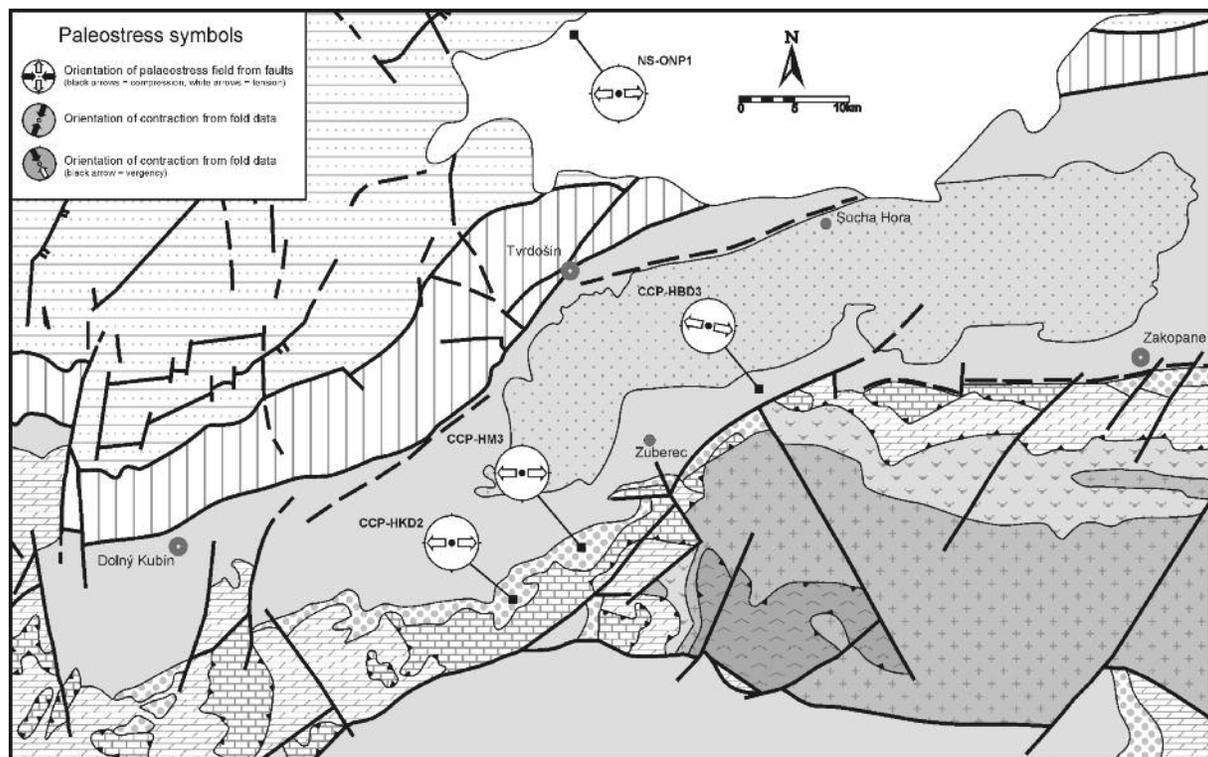
Text-fig. 12. Simplified tectonic map with orientation of palaeostress symbols of the W–E tension (Late Pliocene to Quaternary); see Tables 2 and 3

3d, e; 5d; 9c; 10). The N–S compressional deformation brought about a marked fold evolution predominantly north of the Vysoké Tatry Mts., with unknown vergence. Such fold structures frequently developed during faulting and they are interpreted as drag folds. The N–S shortening caused modification to the E–W elongation of the Podhale Basin, which is arranged into a synclinal structure. The synclinal pattern is confirmed by structural data and by the distribution of the stratigraphical formations (Gross *et al.* 1993; Nemčok *et al.* 1993, 1994; Starek 2001; Pešková 2005). The evolution of the tectonic regime under these conditions began from transpression and passed progressively to transtension up to the Late Miocene.

The maximum principal stress axis σ_1 rotated progressively from N–S to NE–SW during the Late Miocene (Text-figs 3f, g; 5e; 9d; 11). This NNE–SSW compression was also detected by Sperner *et al.* (2002) but those authors dated this tectonic phase as Oligocene(?)–Middle Miocene. However, a more exact age of this deformation phase was established by Tokárová (2004) in the Tatra and Spišská Magura Mts. At the end of this phase, the orientation of the maximum principal stress axis σ_1 also changed gradually from sub-horizontal to subvertical. The post-mid-Miocene NW–SE extension spread into the Western Carpathians by re-activating the extrusion-related strike-slip faults as normal faults (Sperner *et al.* 2002). This last strike-slip tectonic regime was recorded in many sites exposing the Upper Eocene to Lower Miocene sedimentary formations of the CCPB. During this tectonic regime, the Orava–Nowy Targ Basin was formed by a flexural bending of the crust in the Sarmatian during the folding and reverse faulting of the Magura nappe (Roth *et al.* 1963). This process was accompanied by tectonic incorporation of the Oligocene–Miocene sedimentary infill of the marine "piggy-back" basin into the Magura nappe (Roth *et al.* 1963). Pospíšil (1990) assumed that the Orava–Nowy Targ Depression was formed on a mobile belt of the Periklippen zone by a pull-apart mechanism. A similar mechanism for the opening of the Orava–Nowy Targ Basin was also presented by Pomianowski (1995, 2003). The geomorphological evolution and origin of the Orava–Nowy Targ Basin was elaborated by Baumgart-Kotarba (1996, 2001), Baumgart-Kotarba *et al.* (2001).

The youngest tectonic regime is characterised by E–W trending tension which is documented in the Wielka Lipnica sandpit in the Orava–Nowy Targ Basin (Text-figs 3h; 12). The Quaternary stress field in the northern part of the CWC is still uncertain. However, it is assumed that the Quaternary extensional tectonic regime was parallel with the Western Carpathian arc (S_h – minimum horizontal compression axis) and that the S_H (maxi-

mum horizontal compression axis) of the stress field was perpendicular to it; generally N–S (Jarosiński 1998, 2005; Zuchiewicz 1998). These conclusions agree with results from structural measurements carried out in the western part of the CWC (Vojtko *et al.* 2008). The E–W-trending extension in the southern part of the Orava–Nowy Targ was described by Baumgart-Kotarba (2001).

CONCLUSIONS

The history of palaeostress field orientation, from the Late Eocene to the Quaternary, was controlled by the interaction between the Adria microplate and the European Platform. The counterclockwise rotation of the ALCAPA microplate of about 80° (Early Miocene to Middle Badenian rotations) played a dominant role in the orientation of the palaeostress field. However, in the Orava region the spin rotation is still open to question because of a lack of relevant palaeomagnetic data from the study area. The reconstruction of the palaeostress field was carried out by means of fault slip and fold data. Analysis of structural measurements, as well as a geological and structural study of the Orava region shows clockwise rotation of the palaeostress field during the Neogene. One principal phase of rotation of the stress field was distinguished for the Late Eocene to Oligocene, three for the Miocene and one for the Pliocene to (?) Quaternary.

During the Late Eocene to Oligocene, the area was affected by E–W compression. A strike-slip tectonic regime is considered to be the dominant deformational phase. Sedimentation in the CCPB began in the Late Eocene in this area and was controlled by active tectonics documented by sedimentary deformation (Starek 2001; Pešková 2005). This tectonics was observed predominantly in the southeastern part of the CCPB.

This deformational phase was followed by a new, mainly compressional, tectonic regime. Deformation was now characterized by reverse faulting and, to a lesser extent, by strike-slip faulting, which was connected with noticeable evolution of the fold structure. The stress field rotated approximately 40–50° clockwise to the NW–SE position of compression; and the deformational phase is dated as Early Miocene. In reality, the palaeostress field was fixed in the N–S position, while the ALCAPA microplate rotated counterclockwise (Márton *et al.* 1999).

During the Middle and Late Miocene there was a gradual change in the palaeostress orientation and in the character of the tectonic regime. The palaeostress field orientation rotated progressively clockwise from the N–S to the NE–SW position. This is assumed to be real palaeostress rotation, not microplate rotation. Addition-

ally, the tectonic regime passed from transpression through transtension to tension (Text-fig. 4). The Middle Miocene was characterized by a generally N–S-trending compression, and tension perpendicular to it, during a strike-slip tectonic regime. The maximum principal palaeostress axis (σ_1) rotated to the NE–SW position in the Late Miocene. Local fluctuations in the palaeostress field in the northern part of the Central Western Carpathians are probably the consequence of the different rotational history of its internal segments, or are due to inaccurate field measurements.

The youngest tectonic regime (neotectonics) is characterised by E–W-trending tension which has been documented in the Orava–Nowy Targ Basin. The Quaternary tension is parallel to the Western Carpathian arc (S_h), and the S_H of the stress field is generally N–S to NNW–SSE. This extensional tectonic regime was also documented in the Orava region by Chrustek (2005).

Acknowledgement

REFERENCES

Angelier, J. 1979. Determination of the mean principal directions of stress for a given fault population. *Tectonophysics*, **56**, T17–T26.

Angelier, J. 1989. From orientation to magnitudes in paleostress determinations using fault slip data. *Journal of Structural Geology*, **11**, 37–50.

Angelier, J. 1990. Inversion of field data in fault tectonics to obtain the regional stress – III. A new rapid direct inversion method by analytical means. *Geophysical Journal International*, **103**, 363–376.

Angelier, J. 1994. Fault slip analysis and palaeostress reconstruction. In: Hancock P.L. (Ed.), Continental Deformation, pp. 53–100. Pergamon Press, University of Bristol (UK); London.

Bada, G., Fodor, L., Székely, B. and Timár, G. 1996. Tertiary brittle faulting and stress field evolution in the Gerecse Mountains, northern Hungary. *Tectonophysics*, **255**, 269–289.

Balla, Z. 1984. The Carpathian loop and the Pannonian basin. A kinematic analysis. *Geophysical Transactions*, **30**, 313–353.

Baumgart-Kotarba, M. 1996. On origin and age of the Orawa Basin, West Carpathians. *Studia Geomorphologica Carpatho-Balcanica*, **30**, 101–116.

Baumgart-Kotarba, M. 2001a. Continuous tectonic evolution of the Orava Basin (Northern Carpathians) from Late Badenian to the present–day? *Geologica Carpathica*, **52**, 103–110.

Baumgart-Kotarba, M., Dec, J. and Ślusarczyk, R. 2001b. Quaternary tectonic grabens of Wróblówka and Pieniążkowice and their relation to Neogene strata of the Orava Basin and Pliocene sediments of the Domański Wierch series in Podhale, Polish West Carpathians. *Studia Geomorphologica Carpatho-Balcanica*, **35**, 101–119.

Birkenmajer, K. 1986. Stages of structural evolution of the Pieniny Klippen Belt, Carpathians. *Studia Geologica Polonica*, **88**, 7–32.

Bott, M.H.P. 1959. The mechanics of oblique slip faulting. *Geological Magazine*, **96**, 109–117.

Chrustek, M. 2005. Morphotectonics of the Orava Basin, Western Carpathians. *Geolines*, **19**, 26–27.

Csontos, L. 1995. Tertiary tectonic evolution of the Intra-Carpathian area: a review. *Acta Vulcanologica*, **7**, 1–13.

Csontos, L., Nagymarosy, A., Horváth, F. and Kováč, M. 1992. Tertiary evolution of the intracarpathian area: a model. *Tectonophysics*, **208**, 221–241.

Csontos, L., Tari, G., Bergerat, F. and Fodor, L. 1991. Evolution of the stress fields in the Carpatho-Pannonian area during the Neogene. *Tectonophysics*, **199**, 73–91.

Delvaux, D. 1993. The TENSOR program for paleostress reconstruction: examples from the east African and the Baikal rift zones. *Terra Nova*, **5**, supplement. No 1, Proceedings of EUG VII, Strasbourg, 4–8 April, 216.

Delvaux, D. and Sperner, B. 2003. New aspects of tectonic stress inversion with reference to the TENSOR program. In: Nieuwland, D.A. (Ed.), New Insights into Structural Interpretation and Modelling. *Geological Society, London, Special Publications*, **212**, 75–100.

Dupin, J. M., Sassi, W. and Angelier, J. 1993. Homogeneous stress hypothesis and actual fault slip: a distinct element analysis. *Journal of Structural Geology*, **15**, 1033–1043.

Etchecopar, A., Vasseur, G. and Daignieres, M. 1981. An inverse problem in microtectonics for the determination of stress tensor from fault striation analysis. *Journal of Structural Geology*, **3**, 51–65.

Fodor, L. 1995. From transpression to transtension: Oligocene–Miocene structural evolution of the Vienna Basin and the East Alpine–Western Carpathian junction. *Tectonophysics*, **242**, 151–182.

Fodor, L., Magyari, Á., Kázmér, M. and Fogarasi, A. 1992. Gravity-flow dominated sedimentation on the Buda paleoslope (Hungary). Record of Late Eocene continental es-

cape of the Bakony Unit. *Geologische Rundschau,* **81**, 695–716.

Fodor, L., Csontos, L., Bada, G., Györfi, I. and Benkovics, L. 1999. Tertiary tectonic evolution of the Pannonian Basin system and neighbouring orogens: a new synthesis of palaeostress data. In: Durand, B., Jolivet, L., Horváth, F. and Séranne, M. (Eds), The Mediterranean Basins: Tertiary Extension within the Alpine Orogen. *Geological Society*, *London, Special Publications*, **156**, 295–334.

Gapais, D., Cobbold, P. R., Bourgeois, O., Rouby D. and de Urreiztieta M. 2000. Tectonic significance of fault-slip data. *Journal of Structural Geology*, **22**, 881–888.

Golonka, J., Krobicki, M., Oszczypko, N. and Ślączka, A. 2005. Palinspastic modelling and Carpathian Phanerozoic palaeogeographic maps. In: Oszczypko, N., Uchman, A. and Malata, E. (Eds), Palaeotectonic Evolution of the Outer Carpathian and Pieniny Klippen Belt Basins. Instytut Nauk Geologicznych Uniwersytetu Jagiellońskiego, 19–43. Kraków.

Gross, P., Köhler, E., Haško, J., Halouzka, R., Mello, J. and Nagy, A. 1993. Geology of the southern and eastern Orava, 319 pp. Dionýz Štúr Geological Institute; Bratislava. [In Slovak]

Gross, P. Köhler, E. and Samuel, O. 1984. A new lithostratigraphic division of the Inner-Carpathians Paleogene. *Geologické Práce, Správy*, **77**, 75–86. [In Slovak]

Hancock, P.L. 1985. Brittle microtectonics: principles and practice. *Journal of Structural Geology*, **7**, 437–457.

Haško, J. and Polák, M. 1978. Geological map of the Kysucké vrchy and Krivánska Malá Fatra Mts. Dionýz Štúr Geological Institute, Bratislava.

Hók, J., Kováč, M., Kováč, P., Nagy, A. and Šujan, M. 1999. Geology and tectonics of the NE part of the Komjatice Depression. *Slovak Geological Magazine*, **5**, 187–199.

Hók, J., Kováč, M., Rakús, M., Kováč, P., Nagy, A., Kováčová-Slamková, M., Sitár, V. and Šujan, M. 1998. Geologic and tectonic evolution of the Turiec depression in the Neogene. *Slovak Geological Magazine*, **4**, 165–176.

Hók, J., Šimon, L., Kováč, P., Elečko, M., Vass, D. and Halmo, O. 1995. Tectonics of the Hornonitrianska kotlina depression in the Neogene. *Geologica Carpathica*, **46**, 191–196.

Jarosiński M. 1998. Contemporary stress field distortion in the Polish part of the Western Outer Carpathians and their basement. *Tectonophysics,* **297**, 91–119.

Jarosiński M. 2005**.** Ongoing tectonics reactivation of the Outer Carpathians and its impact on the foreland: Results of borehole breakout measurements in Poland. *Tectonophysics,* **410**, 189–216.

Książkiewicz, M. 1977. The tectonics of the Carpathians. In: Pożaryski, W. (Ed.), Geology of Poland, vol. 4. Instytut Geologiczny, Warszawa, pp. 476–620.

Kováč, M. 2000. Geodynamical, palaeogeographical and structural evolution of the Carpathian-Pannonian region during the Miocene: New sight on the Neogene basins of Slovakia. 202 pp. VEDA Publisher; Bratislava. [In Slovak]

Kováč, M., Baráth, I., Holický, I., Marko, F. and Túnyi I. 1989. Basin opening in the Lower Miocene strike-slip zone in the SW part of the Western Carpathians. *Geologický Zborník Geologica Carpathica*, **40**, 37–62.

Kováč, M. and Márton, E. 1998. To rotate or not to rotate: Palinspastic reconstruction of the Carpatho–Pannonian area during the Miocene. *Slovak Geological Magazine*, **4**, 75–85.

Kováč, M., Nagymarosy, A., Soták, J. and Šútovská, K. 1993. Late Tertiary paleogeographic evolution of the Western Carpathians. *Tectonophysics*, **226**, 401–416.

Kováč, M., Kráľ, J., Márton, E., Plašienka, D. and Uher, P. 1994. Alpine uplift history of the Central Western Carpathians: geochronological, paleomagnetic, sedimentary and structural data. *Geologica Carpathica*, **45**, 83–96.

Kováč, P. and Hók, J. 1996. Tertiary development of the western part of the Pieniny Klippen Belt. *Slovak Geological Magazine*, **2**, 137–149.

Lexa, J., Bezák, B., Elečko, M., Eliáš, M., Konečný, V., Less, Gy., Mandl, G. W., Mello, J., Pálenský, P., Pelikán, P., Polák, M., Potfaj, M., Radócz, Gy. Ryłko, W., Schnabel, G. W., Stráník, Z., Vass, D., Vozár, J. and Zelenka, T. 2000: Geological map of Western Carpathians and adjacent areas. Dionýz Štúr Geological Institute, Bratislava.

Maerten, L. 2000. Variation in slip on intersecting normal faults: Implications for paleostress inversion. *Journal of Geophysical Research*, **105** (B11), 25 553–25 565.

Marko, F. 1993. Sense of movement criteria on mesoscale shear fault surfaces (a review). *Mineralia Slovaca*, **25**, 285–287. [In Slovak]

Marko, F. and Kováč, M. 1996. Reconstruction of the Miocene tectonic evolution of the Vaďovce depression based on the analysis of structural and sedimentary record (Western Carpathians). *Mineralia Slovaca*, **28**, 81–91. [In Slovak]

Marko, F. and Vojtko, R. 2006. Structural record and tectonic history of the Mýto-Tisovec fault (Central Western Carpathians). *Geologica Carpathica*, **57**, 211–221.

Marko, F., Fodor, L. and Kováč, M. 1991. Miocene strike-slip faulting and block rotation in Brezovské Karpaty Mts. *Mineralia Slovaca*, **23**, 201–213.

Marko, F., Kováč, M., Fodor, L. and Šútovská, K. 1990. Deformations and kinematics of a Miocene shear zone in the northern part of the Little Carpathians (Buková Furrow, Hrabník Formation). *Mineralia Slovaca*, **22**, 399–410. [In Slovak]

Marko, F., Plašienka, D. and Fodor, L. 1995. Meso–Cenozoic stress field within the Alpine-Carpathian transition zone: A review. *Geologica Carpathica*, **46**, 19–27.

Marko, F., Vojtko, R., Plašienka, D., Sliva, Ľ., Jablonský, J., Reichwalder, P. and Starek, D. 2005. A contribution to the tec-

tonics of the Periklippen zone near Zázrivá (Western Carpathians). *Slovak Geological Magazine*, **11**, 37–43.

Márton, E., Mastella, L. and Tokarski, A.K. 1999. Large Counterclockwise Rotation of the Inner West Carpathian Paleogene Flysch–Evidence from Paleomagnetic Investigations of the Podhale Flysch (Poland). *Physics and Chemistry of the Earth (A)*, **24**, 645–649.

Márton, E., Pagáč, P. and Túnyi, I., 1992. Paleomagnetic investigation on Late Cretaceous–Cenozoic sediments from the NW part of the Pannonian Basin. *Geologica Carpathica*, **43**, 363–368.

Michael, A.J. 1984. Determination of stress from slip data: fault and folds. *Journal of Geophysical Research*, **89**, B13, 11517–11526.

Nagy, A., Vass, D., Petrík, R. and Pereszlényi, M. 1996. Tectonogenesis of the Orava Depression in the light of latest biostratigraphic investigations and organic matter alteration study. *Slovak Geological Magazine*, **2**, 49–58.

Nemčok, J., Bezák, V., Janák, M., Kahan, Š., Ryka, W., Kohút, M., Lehotský, I., Wieczorek, J., Zelman, J., Mello, J., Halouzka, R., Raczkowski, W. and Reichwalder, P. 1993. Explanation of geological map of the Tatra Mountains (1:50,000). GÚDŠ, Bratislava, 135 p. [In Slovak]

Nemčok, J., Bezák, V., Biely, A., Gorek, A., Gross, P., Halouzka, R., Janák, M., Kahan, Š., Kotański, Z., Lefeld, J., Mello, J., Reichwalder, P., Raczkowski, W., Roniewicz, P., Ryka, W., Wieczorek, J. and Zelman, J. 1994. Geological map of the Tatra Mountains. MŽP SR, GÚDŠ, Bratislava.

Nemčok, M. and Nemčok, J. 1994. Late Cretaceous deformation of the Pieniny Klippen Belt, West Carpathians. *Tectonophysics*, **239**, 81–109.

Nieto-Samaniego, A.F. and Alaniz-Alvarez, S.A. 1996. Origin and tectonic interpretation of multiple fault patterns. *Tectonophysics*, **270**, 197–206.

Olszewska, B. and Wieczorek, J. 1998. The Paleogene of the Podhale basin (Polish Inner Carpathians) – micropaleontological perspective. *Przegląd Geologiczny*, **46**, 721–728.

Oszczypko, N. and Ślączka, A., 1989. The evolution of the Miocene basin in the Polish Outer Carpathians and their foreland. *Geologický Zborník*, **40**, 23–37.

Oszczypko, N., Oszczypko-Clowes, M., Golonka, J. and Marko, F. 2005. Oligocene–Lower Miocene sequences of the Pieniny Klippen Belt and adjacent Magura nappe between Jarabina and Poprad River (East Slovakia and South Poland – their tectonic position and paleogeographic implications). *Geological Quarterly*, **49**, 379–402.

Pešková, I. 2005. Terciérna tektonika a paleonapäťová analýza Oravskej kotliny. Manuscript, Diploma thesis, 81 pp. Comenius University; Bratislava.

Petit, J.P. 1987. Criteria for the sense of movement on fault surfaces in brittle rocks. *Journal of Structural Geology*, **9**, 597–608.

Plašienka, D. 1999. Tektochronológia a paleotektonický model jursko – kriedového vývoja Centrálnych Západných Karpát. 125 pp. VEDA Publisher; Bratislava.

Plašienka, D. 2003. Development of basement–involved fold and thrust structures exemplified by the Tatric–Fatric–Veporic nappe system of the Western Carpathians (Slovakia). *Geodinamica Acta*, **16**, 21–38.

Plašienka, D., Grecula, P., Putiš, M., Kováč, M. and Hovorka, D. 1997. Evolution and structure of the Western Carpathians: an overview. In: Grecula P., Hovorka D. and Putiš, M. (Eds), Geological evolution of the Western Carpathians. Mineralia Slovaca–Monograph, Bratislava, 1–24.

Plašienka, D., Soták, J. and Prokešová, R. 1998. Structural profiles across the Šambron-Kamenica Periklippen Zone of the Central Carpathian Paleogene Basin in NE Slovakia. *Mineralia Slovaca*, **29**, 173–184.

Pollard, D.D., Saltzer, S.D. and Rubin, A.M. 1993. Stress inversion method: are they based on faulty assumptions? *Journal of Structural Geology*, **15**, 1045–1054.

Pomianowski P. 1995. Structure of the Orava Basin in the light of selected geophysical data. *Annales Societatis Geologorum Poloniae*, **64**, 67–80. [In Polish with English summary]

Pomianowski P. 2003. Tectonics of the Orava-Nowy Targ Basin – results of the combined analysis of the gravity and geoelectrical data. *Przegląd Geologiczny*, **51**, 498–506.

Pospíšil, L. 1990. The geophysical gravity models of the Orava Neogene basin. *Zemný Plyn a Nafta*, **35**, 301–310. [In Czech]

Ratschbacher, L., Frisch, W., Linzer, H.G. and Merle, O. 1991. Lateral extrusion in the Eastern Alps. Part 2: Structural analysis. *Tectonics*, **10**, 257–271.

Ratschbacher, L., Frisch, W., Linzer, H.-G., Sperner, B., Meschede, M., Decker, K., Nemčok, M., Nemčok, J. and Grygar, R. 1993. The Pieniny Klippen Belt in the Western Carpathians of northeastern Slovakia: structural evidence for transpression. *Tectonophysics*, **226**, 471–483.

Roberts, G.P. and Ganas, A. 2000. Fault-slip directions in central and southern Greece measured from striated and corrugated fault planes: Comparison with focal mechanism and geodetic data. *Journal of Geophysical Research*, **105** (B10), 23 443–23 462.

Roth, Z. (Ed.) 1963. Explanation to geological map at a scale of M 1:200 000, sheet M-34-XX (Trstená). Archive-Geofond; Bratislava. [In Slovak]

Royden, L. 1988. Late Cenozoic tectonics of the Pannonian Basin System. In: Royden, L. and Horváth, F. (Eds), The Pannonian Basin. *Association Americal Petroleum Geologists Memoirs,* **45**, 27–48.

Soták, J. 1998. Central Carpathian Paleogene and its constrains. *Slovak Geological Magazine*, **4**, 203–211.

Soták, J., Bebej, J. and Biroň, A. 1996. Detrital analyse of the Paleogene flysch deposits of the Levoča Mts: evidence for

sources and paleogeography. *Slovak Geological Magazine*, **2**, 345–349.

Soták, J., Pereszlényi, M., Marschalko, R., Milička, J. and Starek, D. 2001. Sedimentology and hydrocarbon habitat of the submarine-fan deposits of the Central Carpathian Paleogene Basin (NE Slovakia), *Marine and Petroleum Geology*, **18**, 87–114.

Soták, J. and Starek, D. 2000. Synorogenic deposition of turbidite fans in the Central-Carpathian Paleogene Basin: evidence for and against sea-level and climatic changes, *Slovak Geological Magazine,* **6**, 191–194.

Sperner B., Ratschbacher L. and Nemčok M. 2002. Interplay between subduction retreat and lateral extrusion: Tectonics of the Western Carpathians. *Tectonics*, **21**, 1028–1051.

Sperner B., Müller B., Heidbach O., Delvaux D., Reinecker J. and Fuchs K. 2003. Tectonic stress of the Earth's crust: advances in the World Stress Map Project. In: Nieuwland D.A. (Ed.), New insights in structural interpretation and modelling. *Geological Society, London, Special Publications*, **212**, 101–128.

Starek D. 2001. Sedimentology and palaeodynamics of the Palaeogene formations in the Central Western Carpathians (Orava region). Manuscript, PhD. Thesis, Geological Institute of the Slovak Academy of Sciences, 152 pp. Bratislava. [In Slovak]

Tari, G., Báldi, T. and Báldi-Beke, M. 1993. Paleogene retroarc flexural basin beneath the Neogene Pannonian Basin: a geodynamic model. *Tectonophysics*, **226**, 433–456.

Tokárová, E. 2004. Structural analysis and palaeostress reconstruction in the Spišská Magura and Podhalie regions. Manuscript, Diploma thesis, 64 pp. Comenius University; Bratislava. [In Slovak]

Twiss, R.J. and Unruh, J.R. 1998. Analysis of fault slip inversions: Do they constrain stress or strain rate? *Journal of Geophysical Research*, **101**, 8335–8361.

Vojtko, R. 2003. Fault slip analysis and geodynamical evolution of the central part of the Slovenské rudohorie Mts. Manuscript, PhD thesis, 91 pp. Comenius University; Bratislava. [In Slovak]

Vojtko, R., Hók, J., Kováč, M., Sliva, Ľ., Joniak, P. and Šujan, M. 2008. Pliocene to Quaternary stress field change in the Western Carpathians (Slovakia). *Geological Quarterly*, **52**, 19–30.

Wagreich, M. 1995. Subduction tectonic erosion and Late Cretaceous subsidence along the northern Austroalpine margin (Eastern Alps, Austria). *Tectonophysics*, **242**, 63–78.

Wallace, R.E. 1951. Geometry of shearing stress and relation to faulting. *Journal of tructural Geology*, **59**, 118–130.

Wallbrecher, E. 1986. Tektonische und gefügeanalytische Arbeitsweisen, 244 pp. Enke; Stuttgart.

Winkler, W. and Slączka, A. 1992. Sediment dispersal and provenance in the Silesian, Dukla, and Magura flysch nappes (Outer Carpathians, Poland). *Geologische Rundschau*, **81**, 371–382.

Zuchiewicz, W. 1998. Cenozoic stress field and jointing in the Outer West Carpathians, Poland. *Journal of Geodynamics*, **26**, 57–68.